Published in final edited form as:
J Med Chem. 2009 April 9; 52(7): 1903–1911. doi:10.1021/jm801344j.

Phenanthrene-based tylophorine-1 (PBT-1) inhibits lung cancer cell growth through the Akt and NF-κB pathways

Jau-Chen Lin[†,#], **Shuenn-Chen Yang**[†,#], **Tse-Ming Hong**[‡], **Sung-Liang Yu**[‡], **Qian Shi**[§], **Linyi Wei**[§], **Hsuan-Yu Chen**[⊥], **Pan-Chyr Yang**[|,*], and **Kuo-Hsiung Lee**[§,*]

†*Institute of Biomedical Sciences, Academia Sinica, No. 128, Academia Road, Sec. 2, NanKang, Taipei, Taiwan*

‡*NTU Center of Genomic Medicine, No, 1, Jen-Ai Road, Sec. 1, Taipei, Taiwan.*

§*Natural Products Research Laboratories, Eshelman School of Pharmacy, University of North Carolina at Chapel Hill, NC27599, USA*

⊥*Institute of Statistical Science, Academia Sinica, No. 128, Academia Road, Sec. 2, NanKang, Taipei, Taiwan*

|*College of Medicine, National Taiwan University, No, 1, Jen-Ai Road, Sec. 1, Taipei, Taiwan.*

Abstract

Tylophorine and related natural compounds exhibit potent antitumor activities. We previously showed that PBT-1, a synthetic C9-substituted phenanthrene-based tylophorine (PBT) derivative, significantly inhibits growth of various cancer cells. In this study, we further explored the mechanisms and potential of PBT-1 as an anticancer agent. PBT-1 dose-dependently suppressed colony formation, induced cell cycle G2/M arrest and apoptosis. DNA microarray and pathway analysis showed that PBT-1 activated the apoptosis pathway and mitogen-activated protein kinase signaling. In contrast, PBT-1 suppressed the nuclear factor kappaB (NF-κB) pathway and focal adhesion. We further confirmed that PBT-1 suppressed Akt activation accelerated RelA degradation via IκB kinase-α, and downregulated NF-κB target gene expression. The reciprocal recruitment of RelA and RelB on *COX-2* promoter region led to downregulation of transcriptional activity. We conclude that PBT-1 induces cell cycle G2/M arrest and apoptosis by inactivating Akt and by inhibiting the NF-κB signaling pathway. PBT-1 may be a good drug candidate for anticancer chemotherapy.

Keywords

Phenanthrene-based tylophorine derivatives; apoptosis; cell cycle arrest; NF-κB; lung cancer

Introduction

Natural products have long been major sources of anticancer and other drugs. Several plants of the *Tylophora* genus have been used medicinally as anti-inflammatory, antiarthritis, and antiamebic agents in East Asia.[1] The phenanthroindolizine alkaloid tylophorine and its analogs are found primarily in plants of the Asclepiadaceae family, including members of the

CORRESPONDING AUTHOR FOOTNOTE: Pan-Chyr Yang, MD, PhD, Department of Internal Medicine, National Taiwan University College of Medicine, No, 1, Sec. 1, Ren-Ai Road, Taipei, Taiwan; Phone:886-2-2356-2185; Fax: 886-2-2322-4793 e-mail: E-mail: pcyang@ntu.edu.tw.
[#]These authors contributed equally to the manuscript
[*]These authors codirected the project and contributed equally

Tylophora genus.[2] Although tylocrebrine, a natural product related to tylophorine, failed in anticancer clinical trials in 1966 because of toxicity to the central nervous system (CNS), certain cytotoxic analogs were reevaluated for antitumor potential by the National Cancer Institute (NCI) using a 60-tumor cell line panel. As we reported previously, a series of novel polar water-soluble synthetic phenanthrene-based tylophorine derivatives (PBTs[a]) exhibit potent cytotoxic activity against the A549 human lung cancer cell line.[3] These compounds may have little or no CNS toxicity because their increased polarity should prevent them from penetrating the blood–brain barrier. Compound PBT-1 showed modest *in vivo* antitumor activity against human A549 xenografts in nude mice and potent *in vitro* cytotoxic activity.[4]

Tylophorine analogs exhibit potent growth-inhibitory activity against a broad range of human cancer cells,[5–10] and this antitumor activity results from the irreversible inhibition of protein synthesis at the elongation stage of the translation cycle.[11–13] Several key metabolic enzymes, including thymidylate synthase[9] and dihydrofolate reductase have been reported as biological targets of tylophorine alkaloids.[8] Tylophorine derivatives also inhibit activator protein-1–mediated, CRE-mediated, and nuclear factor kappaB (NF-κB)-mediated transcription.[14, 15] These discoveries illustrate the potential of tylophorine derivatives as a new class of antitumor drugs. However, the comprehensive evaluation of the antitumor activity of tylophorines has not been reported, and the mechanism responsible for the inhibitory effects on cancer cell growth is largely unknown.

We used cDNA microarray analysis to investigate the antitumor activity of tylophorine analogs against human lung cancer cells and analyzed the effect of PBT-1 on gene expression. Based on the microarray data, we explored the possible signaling pathways that may inhibit cell growth and induce apoptosis. The effects of tylophorine analogs on key signaling pathways were also investigated.

Results

Effect of PBT Series Compounds on Cancer Cell Cytotoxicity

Our previous data showed that novel 9-substituted 2,3-methylenedioxy-6-methoxy-PBTs exhibit potent cytotoxic activity against certain human cancer cell lines, including a multidrug-resistant variant.[4] However, the biological functions of these PBTs have not been explored. To identify the pharmacophores relating to the high potency of the new PBT series, 10 compounds were examined. Their structures are shown in Fig. 1A. The inhibitory effect of the drugs was calculated as the percentage of viable drug-treated cells compared with the percentage of viable cells in the untreated control. The median inhibitory concentration (IC_{50}) value was defined as the concentration of drug that inhibited cell growth by 50%. The CL1-0 lung cancer cell line was exposed to increasing concentrations of compounds for 48 h. PBT-1, PBT-2, PBT-9, and PBT-10 exhibited dose-dependent growth inhibition, with IC_{50} values of 0.81, 0.44, 0.37, and 0.46 μg/mL, respectively, at 48 h (Fig. 1B). The IC_{50} values of the six remaining compounds were > 2 μg/mL; PBT-3, PBT-7, and PBT-8 exhibited greater cytotoxic activity than PBT-4, PBT-5, and PBT-6. These results indicate that the structural features contributing to the greatest cytotoxic effects on lung cancer cells are a pendant pyridine/pyridinium ring with a hydroxymethyl or hydroxyethyl substituent, as found in PBT-1, PBT-2, PBT-9, and PBT-10.

PBT-1 Can Suppress Lung Cancer Cell Growth

To explore the antitumor potential of PBTs, CL1-0, CL1-5, H460, PC-9 and A549 lung cancer cells as well as BEAS2B, immortalized normal bronchial epithelial cells, were treated with the

[a]Abbreviations: PBTs, phenanthrene-based tylophorine derivatives.

highly potent compound PBT-1, and cell viability was determined by the MTS assay. The resulting IC_{50} values for PBT-1 were around 0.2 ~ 0.4 μg/mL against these lung cancer cells but no significant inhibition on BEAS2B cells (Fig. 2A). With increasing concentration of the drug, CL1-0 cells treated with PBT-1 showed cell shrinkage and rounding, followed by broken membranes (Fig. 2B). The inhibitory effect of PBT-1 on the colony formation of CL1-0 cells was calculated as the percentage of visible colonies of the drug-treated groups compared with the percentage in the untreated control groups. Treatment with PBT-1 also suppressed colony formation in a dose-dependent manner. The growth of CL1-0 cells was suppressed fully when the concentration of PBT-1 was > 0.25 μg/mL.

PBT-1 Induces Cell Cycle Arrest in the G2/M Phase and Activates Apoptotic Proteins

To understand the mechanism of PBT-1's effect on cell growth, we used DNA flow cytometry to investigate changes in the cell cycle in CL1-0 cells treated with PBT-1. Treatment with PBT-1 time-dependently decreased the proportion of cells in the G0/G1-phase and increased the proportion of cells in the G2/M-phase up to 12 h (Fig. 3A). Interestingly, a sub-G1 peak and an S-phase peak appeared after 16 h of PBT-1 treatment. To confirm this cell cycle analysis, we measured the effects of PBT-1 on regulatory proteins of cell cycle progression. Western blot analysis indicated that treatment with PBT-1 caused cyclin B1 and cyclin D1 protein accumulation in a dose-dependent manner but had no effect on cyclin A, cyclin E, p21, or p27 protein levels (Fig. 3B). In addition, Annexin V and Western blot analyses indicated that treatment with PBT-1 induced apoptosis of lung cancer cells (Fig. 3C and 3D).

Gene Expression Profiles of Lung Cancer Cells after PBT-1 Treatment

To elucidate the molecular mechanism of PBT-1's induction of cell apoptosis, we used a cDNA microarray with Gene Spring software to analyze the changes in gene expression after PBT-1 treatment. In total, 1437 putative genes showed a statistically significant twofold difference in expression in CL1-0 lung cancer cells after 24 h of PBT-1 treatment (0.5 μg/mL) compared with untreated control cells. Of these 1437 genes, 883 were upregulated and 554 were downregulated. The genes were upregulated or downregulated to a similar extent. The upregulated genes are those involved in signal pathways such as mitogen-activated protein kinase (MAPK); the apoptotic pathway was activated markedly after treatment with PBT-1. In contrast, focal adhesion and metabolic pathway genes were downregulated significantly by treatment with PBT-1. Some of these PBT-1–induced genes are listed and categorized by their putative functions in Table 1. Protein kinase A, CASP8 and FADD-like apoptosis regulator, Tumor necrosis factor receptor 10b, MAPK kinase kinase 14, and NF-κB inhibitor-α were upregulated significantly (twofold) by PBT-1 treatment. The microarray data was also confirmed by real-time RT-PCR.

PBT-1 Can Activate Cell Apoptosis Pathways

To predict the putative signaling pathway involved in PBT-1 stimulation, we used the KEGG and BIOCARTA pathway databases to analyze the differentially expressed profiles of PBT-1–induced genes to fit the transduction-signaling map. Two major pathways were upregulated by PBT-1: the cell cycle regulatory pathway and the apoptotic pathway. Cell cycle analysis showed that PBT-1 increased the expression of cdc25a (2.9-fold) and cyclin D1 (2.1-fold), and decreased the expression of cyclin A (0.33-fold) (Fig. 4A). The results for the apoptosis pathway showed that PDK1 and Akt were downregulated (0.26- and 0.48-fold), and IκB were upregulated (2.2-fold). These data suggest that PBT-1 suppresses the NF-κB signaling pathway by suppressing Akt–IKK activation (Fig. 4B).

PBT-1 Inhibits Akt Phosphorylation and NF-κB Activation

To confirm whether PBT-1 can suppress the activation of both Akt and NF-κB, we used Western blot analysis and an NF-κB reporter assay to examine the changes in Akt and NF-κB activity after PBT-1 treatment. Western blot analysis confirmed that Akt phosphorylation decreased and IκB protein increased in a dose-dependent manner when CL1-0 cells were exposed to increasing PBT-1 concentration (Fig. 5A). The reporter assay showed that NF-κB transcriptional activity was induced by stimulation with TNF-α and that PBT-1 dose-dependently suppressed TNF-α–induced NF-κB transcriptional activity in CL1-0 cells (Fig. 5B). Western blot analysis showed that phosphor-Akt increased after TNF-α treatment but that the TNF-α–induced activation of Akt was inhibited by PBT-1 in both CL1-0 and A549 cells (Fig. 5C). In addition, RelA and IκB protein decreased when the cells were cotreated with TNFα and PBT-1. The expression level of COX-2, a gene known to be downstream of NF-κB, was high in cells treated with TNF-α, but its expression decreased in cells exposed to PBT-1. Interestingly, the activity of IKKα, but not IKKβ, increased after treatment with PBT-1 (Fig. 5D). The chromatin IP assay showed a decreased binding affinity of RelA and NF-κB1 (p50) to the NF-κB response element on the COX-2 promoter in A540 cells. In contrast, the binding activity of ReIB was higher after exposure to PBT-1 co-treated with TNF-α than after exposure to TNF-α alone, but the binding activity of ReIB decreased when exposed to PBT-1 at a concentration > 0.25 μg/mL (Fig. 5E).

Discussion

In this study, we demonstrated that the PBT analog PBT-1 has potent cytotoxicity against various lung cancer cells and can induce cell cycle G2/M arrest and apoptosis. The microarray data showed that PBT-1 increases the expression of genes belonging to certain signaling pathways, such MAPK and apoptosis, and dramatically suppresses the expression of genes for metabolic enzyme. These data indicate that PBT-1 treatment can regulate these signaling pathways. We showed further that the key signaling pathways affected in lung cancer cell survival involve inactivation of Akt and NF-κB. Our data suggest that PBT-1 affects cell growth by inhibiting the NF-κB signaling pathway. This suggests that PBT-1 is a good candidate for anticancer therapy.

Tylophorine compounds comprise a new class of anticancer agents because of their novel chemical structure combined with the unique spectrum of activity compared with current antitumor drugs, based on NCI tumor cell panel studies. Because a related compound, tylocrebrine, failed in clinical trials because of CNS toxicity, investigators have since tried to develop derivatives that are not toxic to the CNS. We designed and synthesized a series of novel 9-substituted 2,3-methylenedioxy-6-methoxy-PBTs, and one analog (PBT-1) showed in vivo activity in a murine model without overt toxicity to the animals.[3, 4] The biological function and molecular mechanism responsible for the effect of PBT-1 on cell cytotoxicity merit investigation. Interestingly, CL1-0 and CL1-5 cells, which were both isolated from the same original clinical sample, exhibited the same sensitivity (IC_{50}) to PBT-1, even though they have different intensities of invasive ability. This suggests that the key mechanism responsible for PBT-1's ability to suppress cell growth is involved in tumorigenesis but not in the invasion machinery.

To elucidate the mechanism of action of PBT-1, we examined its effect on cell cycle progression. We found that PBT-1 induced G2/M arrest, which was accompanied by accumulation of cyclin B1 (Fig. 2) and activation of the MAPK signaling pathway, as predicted by our microarray data (Table 1). Interestingly, paclitaxel also induces cyclin B1 accumulation,[16] cell cycle G2/M arrest, and apoptosis through an MAPK-dependent pathway.[17] Thus, PBT-1 and paclitaxel may activate the same death-signaling pathway to induce cell apoptosis. Gao et al. found a dose-dependent S-phase accumulation at 24 h in human nasopharyngeal

carcinoma KB cells treated with another tylophorine analog class (DCBs) developed by their laboratory.[15] They also demonstrated that, in human pancreatic duct carcinoma cells, the percentage of G2/M-phase cells increased gradually with time of exposure to a tylophorine analog, whereas the percentage of S-phase cells increased initially and then decreased with exposure time.[18] We found that PBT-1 treatment increased the percentage of G2/M-phase cells at 12 h, but this was followed by a decreased percentage of G2/M-phase cells and a corresponding increased percentage of S-phase cells after 16 h. These contrasting effects may relate to the variant behavior of cell types and differences in the particular tylophorine analogs. However, our microarray data also suggest that these compounds decrease cell growth by interrupting the regulatory proteins in cell cycle progression (Fig. 4B).

NF-κB is a key transcription factor for the inflammatory response,[19] tumor progression,[20] and drug resistance.[21, 22] Suppression of NF-κB activity leads to induction of an apoptotic response.[23] Thus, NF-κB is an important therapeutic target in cancer treatment.[24] Using a cDNA microarray technique, we found that treatment of cells with PBT-1 led to downregulation of Akt and upregulation of IκB. These results suggest two possible mechanisms: 1) that there is a link between Akt inactivation and IκB accumulation and 2) that NF-κB activity may be suppressed by PBT-1 treatment because of IκB accumulation. IKK regulates IκB degradation by phosphorylation, and IKK activity is regulated by Akt.[25, 26] Thus, suppression of Akt by PBT-1 treatment could explain why IκB can escape protein degradation and accumulate in the cytoplasm.

The abundant dephosphorylated IκB can bind NF-κB to block its translocation from the cytoplasm to nucleus so that downstream genes of NF-κB, such as COX-2, cannot be expressed. Contrary to expectation, we found that PBT-1 can upregulate but cannot suppress the expression of IKKα and its phosphorylation. Lawrence *et al*. demonstrated that IKKα can suppress NF-κ activity by accelerating both the turnover of NF-κB subunits RelA and c-Rel, and their removal from proinflammatory gene promoters, resulting in the resolution of inflammation in macrophages.[27] These results are consistent with our finding that RelA degradation correlated with the increasing expression of IKKα upon treatment with PBT-1. Interestingly, our data showed that RelB, a downstream gene of IKKα, was also activated by PBT-1treatment (Fig. 5). Other studies demonstrated that RelB plays a role in endotoxin (lipopolysaccharide)-induced tolerance and anti-inflammatory effects through the reciprocal recruitment of RelA and RelB to NF-κB target gene promoters, resulting in the downregulation of NF-κB target genes.[28, 29] Taken together, these results indicate that PBT-1 may activate an alternative NF-κB pathway to inhibit the canonical NF-κB pathway induced by proinflammatory cytokines by activating IKKα.[30] This novel finding provides a unique perspective on the traditional anti-inflammatory and antiarthritis uses of Tylophora alkaloids; namely, that these compounds can remit the symptoms of asthma and inflammation by activating the IKKα–RelB pathway to tolerate the immune response induced by environmental stimulation, as well as autoimmune diseases. However, this hypothesis needs to be further studied.

Akt (protein kinase B) has been identified as a downstream target of growth factor receptor activation, such as by insulin-like growth factor, epidermal growth factor, basic fibroblast growth factor, insulin, interleukin-6, and macrophage colony stimulating factor.[31–33] Akt controls vital cellular functions such as cell survival, cell cycle progression, and glucose metabolism. The Akt gene is overexpressed and is constitutively active in many human cancers.[34–39] Bad, a proapoptotic member of the Bcl-2 family, is a substrate of Akt, which can phosphorylate Bad significantly at Ser^{136} and then inhibit its proapoptotic functions.[40, 41] Inactivation of Akt is considered an attractive approach for chemotherapy. Recent studies have shown that inhibition of Akt alone or in combination with other cancer chemotherapeutics can reduce the threshold of apoptosis and kill cancer cells.[42, 43] We found that PBT-1 can suppress

inducible activation of Akt in lung cancer cells. Intriguingly, the inactivation of Akt by PBT-1 treatment correlated with the downregulation of COX-2 but not with IKK activity. This suggests that PBT-1, a novel Akt inhibitor, can regulate the Akt-dependent regulation of NF-κB through other mediators, such as mTOR, which regulates IKK activity.[44] The mechanism for this action remains unclear. Taken together, our data show that PBT-1 may be a highly promising, anticancer drug that suppresses cancer cell growth by inhibiting Akt and NF-κB activity. However, the detailed molecular mechanism of this PBT-1–related suppression of Akt activation and NF-κB requires further investigation.

In conclusion, we have shown that PBT-1 can induce cell cycle G2/M arrest and apoptosis by interrupting the regulatory proteins in cell cycle progression and by inhibiting the NF-κB signaling pathway by inactivating Akt. This new class of tylophorine compounds has a unique mode of action that differs from that of other known antitumor compounds. PBT-1 or a future analog will be a good candidate for a new agent for anticancer therapy.

Experimental Section

Cell Lines

The human lung adenocarcinoma cell lines CL1-0 and CL1-5 were established in our laboratory,[45, 46] and with A549 cells (American Type Culture Collection CCL-185) were grown in normal RPMI 1640 culture medium (GIBCO-Life Technologies, Inc., Gaithersburg, MD) or Dulbecco's modified Eagle's medium (GIBCO-Life Technologies), supplemented with 1.5 g/L of $NaHCO_3$, 4.5 g/L glucose, and 10% fetal bovine serum (FBS; GIBCO-Life Technologies). Tumor necrosis factor-α(TNF-α) was purchased from Peprotech (Rocky Hill, NJ). H460, PC-9 and BEAS2B cells were gifted from Dr. Ker-Chau Li, Dr. Chih-Hsin Yang and Dr. Reen Wu, respectively.

Compounds

Ten tested phenanthrene-based derivatives (PBT-1–PBT-10) were synthesized by Dr. KH Lee's laboratory.[3, 4]

Cell Proliferation Assay

Cell proliferation was measured by using a CellTiter 96 Aqueous Non-radioactive Cell Proliferation Assay kit (Promega, Madison, WI). Cells were transferred in four replicates to a 96-well plate at a concentration of 2×10^3 cells/well in 100 μL of complete RPMI 1640 with or without the drugs. The cells were incubated at 37 °C in 5% CO_2 for 48 h, the viability of the cells was analyzed after the addition of 3-(4,5-dimethylthiazol-2-yl)-5-(3-carboxymethoxyphenyl)-2-(4-sulfophenyl)-2H-tetrazolium (MTS) reagent to the cultured cells, and the cells were lysed according to the manufacturer's instructions. Absorbance was determined using Emax microplate reader (Molecular Devices, Union City, CA) at a wavelength of 490 nm.

Colony Formation Assay

Cells (5×10^2/well) were plated in six-well plates. After 24 h, cells were exposed to serial dilutions of the drugs for the times indicated. Five hundred or 1,000 viable cells were plated in triplicate in six-well plates, grown for 10 to 14 days, fixed, and stained with 0.5% methylene blue in 50% ethanol for 1 h. The plates were washed and dried, and the colonies were counted to obtain a cloning efficiency for each drug concentration.

Cell Cycle Analysis

A total of 2×10^5 CL1-0 cells/dish were seeded onto each 60 mm dish and incubated for 24 hours. Various concentrations of PBT-1 were added to the culture media and the cells were incubated for an additional 2, 6, 12, 16, and 24 h. Cells were harvested and fixed in cold 70% ethanol at 4 °C for 16 h and incubated with 20 μg/mL of RNase A at 37 °C for 30 min and then with 50 μg/mL of propidium iodide (PI) at 4 °C for 30 min. Samples were analyzed immediately by flow cytometry (BD Biosciences, San Jose, CA). The cell cycle phase distribution was determined using CellQuest software (BD Biosciences).

Western Blot Analysis

Equal amounts (50 μg) of cell lysate were separated by 10% SDS–PAGE, and transferred to a polyvinylidene membrane (Millipore, Billerica, MA). The membrane was probed with antibodies directed against cyclin A (Santa Cruz Biotechnology, Santa Cruz, CA), cyclin B1, cyclin D1, cyclin E, p21, p27, RelA, p-Akt, Akt, IκB kinase α (IKKα), p-IKKα/β, and α-actin (all from Sigma, St Louis, MO). Antibodies were diluted in TBS (pH 7.5) containing 0.05% (v/v) Tween 20 and 5% (w/v) dried milk. Blots were incubated with the appropriate horseradish peroxidase-conjugated secondary antibodies (Amersham Biosciences, Uppsala, Sweden). Bound antibodies were visualized by electrochemical luminescence staining with autoradiographic detection using Kodak X-Omat Blue film (PerkinElmer Life Science, Boston, MA).

Apoptosis Assay

Control or treated cells were resuspended in Annexin-binding buffer, stained with Alexa Fluor 488 Annexin V or PI,[42] and incubated at room temperature for 15 min. The cells stained only with Annexin V were used as the positive control to set the apoptotic window, and the cells stained only with PI were used as the positive control to set the necrotic window. Double-stained, formaldehyde-treated cells were mainly necrotic. The acquired data were analyzed using CellQuest software (BD Biosciences).

DNA Microarray Analysis

The detailed protocol for the human DNA microarray analysis has been reported in our previous studies.[47, 48] Total RNA was extracted from the CL1-0 cells incubated with or without the drugs using RNAzol B solution (Life Tech, Gaithersburg, MD), and the mRNA was extracted using an mRNA isolation kit (Qiagen, Hilden, Germany), according to the manufacturer's protocol. Five micrograms of mRNA from each sample was used in each array. The microarray images were scanned, digitized, and analyzed using a flatbed scanner (PowerLook 3000; UMAX, Taipei, Taiwan) and GenePix 3.0 software (Axon Instruments, Union City, CA). When designing the microarray experiments, we adhered to the guidelines of the Microarray Gene Expression Data Society (www.mged.org/Workgroups/MIAME/miame_checklist.html).

Identification of Pathways Using the KEGG and BioCarta Databases

Gene identification was performed to determine which biochemical pathways were altered during treatment with PBT-1. Having identified genes on the basis of the cDNA microarray data, we were also interested in determining whether any of these genes were part of the same pathway. Accordingly, we searched the Kyoto Encyclopedia of Genes and Genomes (KEGG) (http://www.genome.ad.jp/kegg/pathway.html) and the BioCarta (http://www.biocarta.com/genes/allpathways.asp) biochemical pathway database using the genes selected from cDNA microarray analysis described previously.[49]

Real-Time quantitative RT-polymerase chain reaction

To validate the microarray data, real-time quantitative RT-PCR was performed according to our previous described method.[48] Primers were performed as listed on Table 1. All reactions were carried in 20 μl volumes containing 10 μl of iTaqTM Fast SYBR Green Supermix with ROX (Bio-Rad, Hercules, CA). GAPDH was performed as internal control.

Transient Transfection and Luciferase Activity

Adherent cells (1×10^5) cells in six-well plates were transiently transfected with 0.2 μg of a pNf-κB-Luc vector (Stratagene, La Jolla, CA) and 1 μg of pSV-β-galactosidase vector dissolved in 10 μL lipofectamine (Invitrogen, Carlsbad, CA) as the internal control. The plasmids were transfected according to the manufacturer's instructions. After 20 h, the medium was changed to serum-free medium, the cells were pretreated with increasing concentrations of PBT-1 as indicated for 1 h, and the cells were stimulated with various concentrations of TNF-α as indicated for 4 h. Cell extracts were harvested using 250 μL of lysis buffer (Tropix, Inc., Bedford, MA) per well. To measure the luciferase and β-galactosidase activities, cell extracts (20 μL each) were assayed separately using the Luciferase Assay Kit and Galacto-Light Plus™ system (Tropix, Inc.), respectively. Luciferase activity was measured and analyzed using an FB12 luminometer (Zylux Corporation, Oak Ridge, TN).

Chromatin Immunoprecipitation (ChIP) Assay

The chromatin immunoprecipitation assay has been described previously.[50] Briefly, A549 cells were cross-linked with 1% formaldehyde and the reaction was stopped with 0.125 M glycine. The cells were solved in 250 μL of cell lysis buffer. The pelleted nuclei were suspended in 150 μL of nuclei lysis buffer and diluted with immunoprecipitation (IP) dilution buffer. The samples were sonicated at 12 W for 45 s. The DNA–protein supernatant was reacted with anti-RelA (Santa Cruz), anti-p50, and anti-RelB antibodies at 4 °C overnight. The immunoprecipitated complexes were collected with protein A/G Sepharose beads (Sigma) and then washed sequentially with low-salt wash buffer, high-salt wash buffer, LiCl wash buffer, and Tris-EDTA buffer. The precipitates were eluted with elution buffer (1% SDS, 100 mM $NaHCO_3$). To reverse the cross-linking, 5 M NaCl and RNase were added, and the samples were incubated at 65 °C overnight. The extracted DNA was analyzed by polymerase chain reaction (PCR) using primers spanning the proximal (nt +87 to +106) or distal (nt −340 to −359) regions of human COX-2.[51] After 35 cycles of amplification, the PCR products were run on a 2% agarose gel and visualized with ethidium bromide staining.

Statistical Analysis

Our previous studies provide detailed descriptions and discussion of the issues involved in generating the microarray data, data normalization, and statistical analysis and interpretation.[47, 52] Genes that were upregulated or downregulated in response to PBT-1 treatment were identified and used for pathway analysis. An upregulated gene had to show a 2-fold increase in the cDNA microarray. These genes were analyzed further by our in-house data-mining tool based on KEGG and BIOCARTA pathway databases (http://biochip.nchu.edu.tw/SpecificDB/mouse.html).

Acknowledgment

This investigation was supported by grant DOH97-TD-G-111-018 from National Research Program for Genomic Medicine (PC Yang) and grant CA-17625 from the National Cancer Institute, NIH (KH Lee).

REFERENCES

1. Wu PL, Rao KV, Su CH, Kuoh CS, Wu TS. Phenanthroindolizidine alkaloids and their cytotoxicity from the leaves of Ficus septica. Heterocycles 2002;57:2401–2408.
2. Li Z, Jin Z, Huang R. Isolation, Total Synthesis and Biological Activity of Phenanthroindolizidine and Phenanthroquinolizidine Alkaloids. Synthesis 2001;16:2365–2378.
3. Wei L, Brossi A, Kendall R, Bastow KF, Morris-Natschke SL, Shi Q, Lee KH. Antitumor agents 251: synthesis, cytotoxic evaluation, and structure-activity relationship studies of phenanthrene-based tylophorine derivatives (PBTs) as a new class of antitumor agents. Bioorg Med Chem 2006;14:6560–6569. [PubMed: 16809043]
4. Wei L, Shi Q, Bastow KF, Brossi A, Morris-Natschke SL, Nakagawa-Goto K, Wu TS, Pan SL, Teng CM, Lee KH. Antitumor agents 253. Design, synthesis, and antitumor evaluation of novel 9-substituted phenanthrene-based tylophorine derivatives as potential anticancer agents. J Med Chem 2007;50:3674–3680. [PubMed: 17585747]
5. Staerk D, Lykkeberg AK, Christensen J, Budnik BA, Abe F, Jaroszewski JW. In vitro cytotoxic activity of phenanthroindolizidine alkaloids from Cynanchum vincetoxicum and Tylophora tanakae against drug-sensitive and multidrug-resistant cancer cells. J Nat Prod 2002;65:1299–1302. [PubMed: 12350151]
6. Ganguly T, Khar A. Induction of apoptosis in a human erythroleukemic cell line K562 by tylophora alkaloids involves release of cytochrome c and activation of caspase 3. Phytomedicine 2002;9:288–295. [PubMed: 12120809]
7. Komatsu H, Watanabe M, Ohyama M, Enya T, Koyama K, Kanazawa T, Kawahara N, Sugimura T, Wakabayashi K. Phenanthroindolizidine alkaloids as cytotoxic substances in a Danaid butterfly, Ideopsis similis, against human cancer cells. J Med Chem 2001;44:1833–1836. [PubMed: 11356117]
8. Rao KN, Venkatachalam SR. Inhibition of dihydrofolate reductase and cell growth activity by the phenanthroindolizidine alkaloids pergularinine and tylophorinidine: the in vitro cytotoxicity of these plant alkaloids and their potential as antimicrobial and anticancer agents. Toxicol In Vitro 2000;14:53–59. [PubMed: 10699361]
9. Rao KN, Bhattacharya RK, Venkatachalam SR. Inhibition of thymidylate synthase and cell growth by the phenanthroindolizidine alkaloids pergularinine and tylophorinidine. Chem Biol Interact 1997;106:201–212. [PubMed: 9413547]
10. Rao KV, Wilson RA, Cummings B. Alkaloids of tylophora. 3. New alkaloids of Tylophora indica (Burm) Merrill and Tylophora dalzellii Hook. f. J Pharm Sci 1971;60:1725–1726. [PubMed: 5133930]
11. Gupta RS, Siminovitch L. Mutants of CHO cells resistant to the protein synthesis inhibitors, cryptopleurine and tylocrebrine: genetic and biochemical evidence for common site of action of emetine, cryptopleurine, tylocrebine, and tubulosine. Biochemistry 1977;16:3209–3214. [PubMed: 560858]
12. Huang MT, Grollman AP. Mode of action of tylocrebrine: effects on protein and nucleic acid synthesis. Mol Pharmacol 1972;8:538–550. [PubMed: 4343427]
13. Donaldson GR, Atkinson MR, Murray AW. Inhibition of protein synthesis in Ehrlich ascites-tumour cells by the phenanthrene alkaloids tylophorine, tylocrebrine and cryptopleurine. Biochem Biophys Res Commun 1968;31:104–109. [PubMed: 4869942]
14. Gao W, Chen AP, Leung CH, Gullen EA, Furstner A, Shi Q, Wei L, Lee KH, Cheng YC. Structural analogs of tylophora alkaloids may not be functional analogs. Bioorg Med Chem Lett 2008;18:704–709. [PubMed: 18077159]
15. Gao W, Lam W, Zhong S, Kaczmarek C, Baker DC, Cheng YC. Novel mode of action of tylophorine analogs as antitumor compounds. Cancer Res 2004;64:678–688. [PubMed: 14744785]
16. Ling YH, Consoli U, Tornos C, Andreeff M, Perez-Soler R. Accumulation of cyclin B1, activation of cyclin B1-dependent kinase and induction of programmed cell death in human epidermoid carcinoma KB cells treated with taxol. Int J Cancer 1998;75:925–932. [PubMed: 9506539]
17. Bacus SS, Gudkov AV, Lowe M, Lyass L, Yung Y, Komarov AP, Keyomarsi K, Yarden Y, Seger R. Taxol-induced apoptosis depends on MAP kinase pathways (ERK and p38) and is independent of p53. Oncogene 2001;20:147–155. [PubMed: 11313944]

18. Shiah HS, Gao W, Baker DC, Cheng YC. Inhibition of cell growth and nuclear factor-kappaB activity in pancreatic cancer cell lines by a tylophorine analogue, DCB-3503. Mol Cancer Ther 2006;5:2484–2493. [PubMed: 17041092]
19. Sen R, Baltimore D. Multiple nuclear factors interact with the immunoglobulin enhancer sequences. Cell 1986;46:705–716. [PubMed: 3091258]
20. Huber MA, Azoitei N, Baumann B, Grunert S, Sommer A, Pehamberger H, Kraut N, Beug H, Wirth T. NF-kappaB is essential for epithelial-mesenchymal transition and metastasis in a model of breast cancer progression. J Clin Invest 2004;114:569–581. [PubMed: 15314694]
21. Baldwin AS. Control of oncogenesis and cancer therapy resistance by the transcription factor NF-kappaB. J Clin Invest 2001;107:241–246. [PubMed: 11160144]
22. Wang CY, Cusack JC Jr, Liu R, Baldwin AS Jr. Control of inducible chemoresistance: enhanced anti-tumor therapy through increased apoptosis by inhibition of NF-kappaB. Nat Med 1999;5:412–417. [PubMed: 10202930]
23. Bharti AC, Aggarwal BB. Nuclear factor-kappa B and cancer: its role in prevention and therapy. Biochem Pharmacol 2002;64:883–888. [PubMed: 12213582]
24. Kim HJ, Hawke N, Baldwin AS. NF-kappaB and IKK as therapeutic targets in cancer. Cell Death Differ 2006;13:738–747. [PubMed: 16485028]
25. Romashkova JA, Makarov SS. NF-kappaB is a target of AKT in anti-apoptotic PDGF signalling. Nature 1999;401:86–90. [PubMed: 10485711]
26. Ozes ON, Mayo LD, Gustin JA, Pfeffer SR, Pfeffer LM, Donner DB. NF-kappaB activation by tumour necrosis factor requires the Akt serine-threonine kinase. Nature 1999;401:82–85. [PubMed: 10485710]
27. Lawrence T, Bebien M, Liu GY, Nizet V, Karin M. IKKalpha limits macrophage NF-kappaB activation and contributes to the resolution of inflammation. Nature 2005;434:1138–1143. [PubMed: 15858576]
28. Saccani S, Pantano S, Natoli G. Modulation of NF-kappaB activity by exchange of dimers. Mol Cell 2003;11:1563–1574. [PubMed: 12820969]
29. Xia Y, Pauza ME, Feng L, Lo D. RelB regulation of chemokine expression modulates local inflammation. Am J Pathol 1997;151:375–387. [PubMed: 9250151]
30. Lawrence T, Bebien M. IKKalpha in the regulation of inflammation and adaptive immunity. Biochem Soc Trans 2007;35:270–272. [PubMed: 17371257]
31. Talapatra S, Thompson CB. Growth factor signaling in cell survival: implications for cancer treatment. J Pharmacol Exp Ther 2001;298:873–878. [PubMed: 11504779]
32. Datta SR, Brunet A, Greenberg ME. Cellular survival: a play in three Akts. Genes Dev 1999;13:2905–2927. [PubMed: 10579998]
33. Downward J. Mechanisms and consequences of activation of protein kinase B/Akt. Curr Opin Cell Biol 1998;10:262–267. [PubMed: 9561851]
34. Roy HK, Olusola BF, Clemens DL, Karolski WJ, Ratashak A, Lynch HT, Smyrk TC. AKT proto-oncogene overexpression is an early event during sporadic colon carcinogenesis. Carcinogenesis 2002;23:201–205. [PubMed: 11756242]
35. Brognard J, Clark AS, Ni Y, Dennis PA. Akt/protein kinase B is constitutively active in non-small cell lung cancer cells and promotes cellular survival and resistance to chemotherapy and radiation. Cancer Res 2001;61:3986–3997. [PubMed: 11358816]
36. Liu W, Li J, Roth RA. Heregulin regulation of Akt/protein kinase B in breast cancer cells. Biochem Biophys Res Commun 1999;261:897–903. [PubMed: 10441522]
37. Lynch HT, Casey MJ, Lynch J, White TE, Godwin AK. Genetics and ovarian carcinoma. Semin Oncol 1998;25:265–280. [PubMed: 9633840]
38. Miwa W, Yasuda J, Murakami Y, Yashima K, Sugano K, Sekine T, Kono A, Egawa S, Yamaguchi K, Hayashizaki Y, Sekiya T. Isolation of DNA sequences amplified at chromosome 19q13.1-q13.2 including the AKT2 locus in human pancreatic cancer. Biochem Biophys Res Commun 1996;225:968–974. [PubMed: 8780719]
39. Staal SP. Molecular cloning of the akt oncogene and its human homologues AKT1 and AKT2: amplification of AKT1 in a primary human gastric adenocarcinoma. Proc Natl Acad Sci U S A 1987;84:5034–5037. [PubMed: 3037531]

40. del Peso L, Gonzalez-Garcia M, Page C, Herrera R, Nunez G. Interleukin-3-induced phosphorylation of BAD through the protein kinase Akt. Science 1997;278:687–689. [PubMed: 9381178]
41. Datta SR, Dudek H, Tao X, Masters S, Fu H, Gotoh Y, Greenberg ME. Akt phosphorylation of BAD couples survival signals to the cell-intrinsic death machinery. Cell 1997;91:231–241. [PubMed: 9346240]
42. Weng SC, Kashida Y, Kulp SK, Wang D, Brueggemeier RW, Shapiro CL, Chen CS. Sensitizing estrogen receptor-negative breast cancer cells to tamoxifen with OSU-03012, a novel celecoxib-derived phosphoinositide-dependent protein kinase-1/Akt signaling inhibitor. Mol Cancer Ther 2008;7:800–808. [PubMed: 18413793]
43. Suzuki E, Umezawa K, Bonavida B. Rituximab inhibits the constitutively activated PI3K-Akt pathway in B-NHL cell lines: involvement in chemosensitization to drug-induced apoptosis. Oncogene 2007;26:6184–6193. [PubMed: 17420722]
44. Dan HC, Cooper MJ, Cogswell PC, Duncan JA, Ting JP, Baldwin AS. Akt-dependent regulation of NF-{kappa}B is controlled by mTOR and Raptor in association with IKK. Genes Dev 2008;22:1490–1500. [PubMed: 18519641]
45. Chen JJ, Peck K, Hong TM, Yang SC, Sher YP, Shih JY, Wu R, Cheng JL, Roffler SR, Wu CW, Yang PC. Global analysis of gene expression in invasion by a lung cancer model. Cancer Res 2001;61:5223–5230. [PubMed: 11431363]
46. Chu YW, Yang PC, Yang SC, Shyu YC, Hendrix MJ, Wu R, Wu CW. Selection of invasive and metastatic subpopulations from a human lung adenocarcinoma cell line. Am J Respir Cell Mol Biol 1997;17:353–360. [PubMed: 9308922]
47. Yu SL, Chen HW, Yang PC, Peck K, Tsai MH, Chen JJ, Lin FY. Differential gene expression in gram-negative and gram-positive sepsis. Am J Respir Crit Care Med 2004;169:1135–1143. [PubMed: 15001460]
48. Chen HW, Yu SL, Chen WJ, Yang PC, Chien CT, Chou HY, Li HN, Peck K, Huang CH, Lin FY, Chen JJ, Lee YT. Dynamic changes of gene expression profiles during postnatal development of the heart in mice. Heart 2004;90:927–934. [PubMed: 15253972]
49. Kanehisa M, Goto S, Kawashima S, Nakaya A. The KEGG databases at GenomeNet. Nucleic Acids Res 2002;30:42–46. [PubMed: 11752249]
50. Wu CC, Lin JC, Yang SC, Lin CW, Chen JJ, Shih JY, Hong TM, Yang PC. Modulation of the expression of the invasion-suppressor CRMP-1 by cyclooxygenase-2 inhibition via reciprocal regulation of Sp1 and C/EBP{alpha}. Mol Cancer Ther 2008;7:1365–1375. [PubMed: 18524846]
51. Miao F, Gonzalo IG, Lanting L, Natarajan R. In vivo chromatin remodeling events leading to inflammatory gene transcription under diabetic conditions. J Biol Chem 2004;279:18091–18097. [PubMed: 14976218]
52. Chen JJ, Lin YC, Yao PL, Yuan A, Chen HY, Shun CT, Tsai MF, Chen CH, Yang PC. Tumor-associated macrophages: the double-edged sword in cancer progression. J Clin Oncol 2005;23:953–964. [PubMed: 15598976]

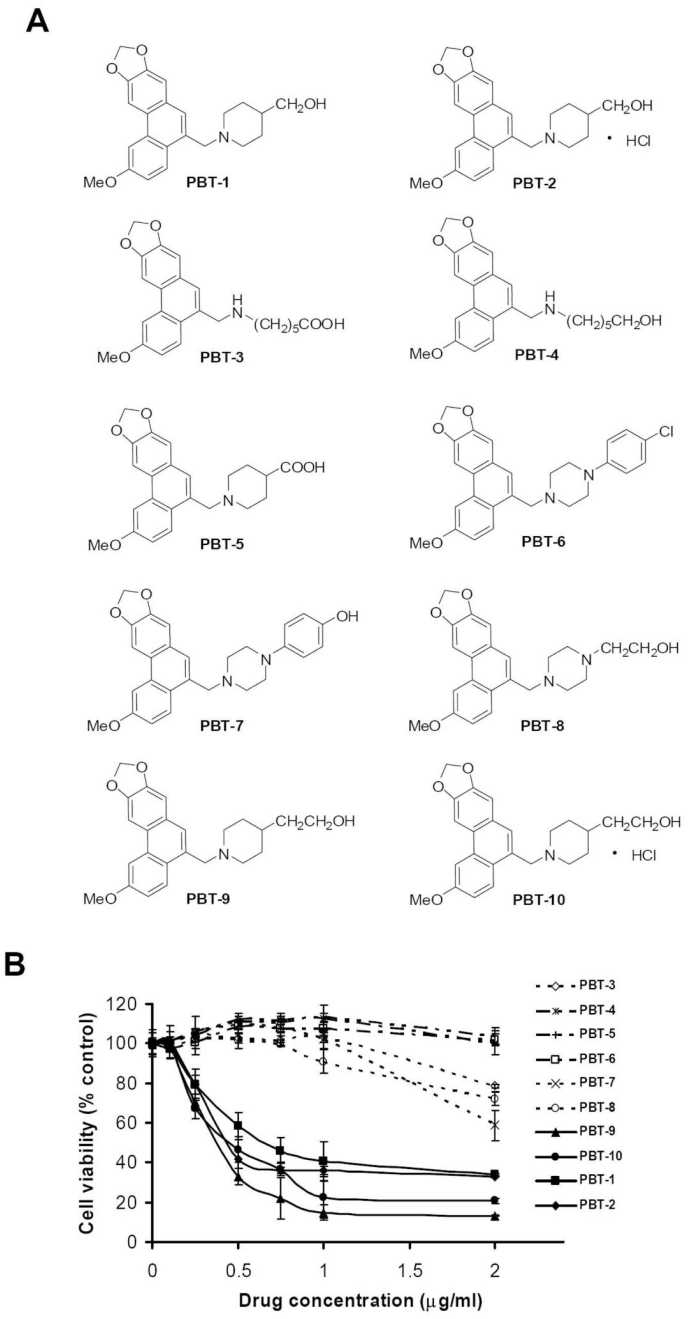

Figure 1. Structure and cytotoxic activity of PBT-series compounds in lung cancer cells

(A) Chemical structures of PBT compounds. (B) CL1-0 cells were treated with various PBT compounds as indicated for 48 h. The viable cells were detected with an MTS assay. PBT-1, PBT-2, PBT-9, and PBT-10 exhibited dose-dependent growth inhibition, and the IC_{50} values were 0.81, 0.44, 0.37, and 0.46 μg/mL, respectively.

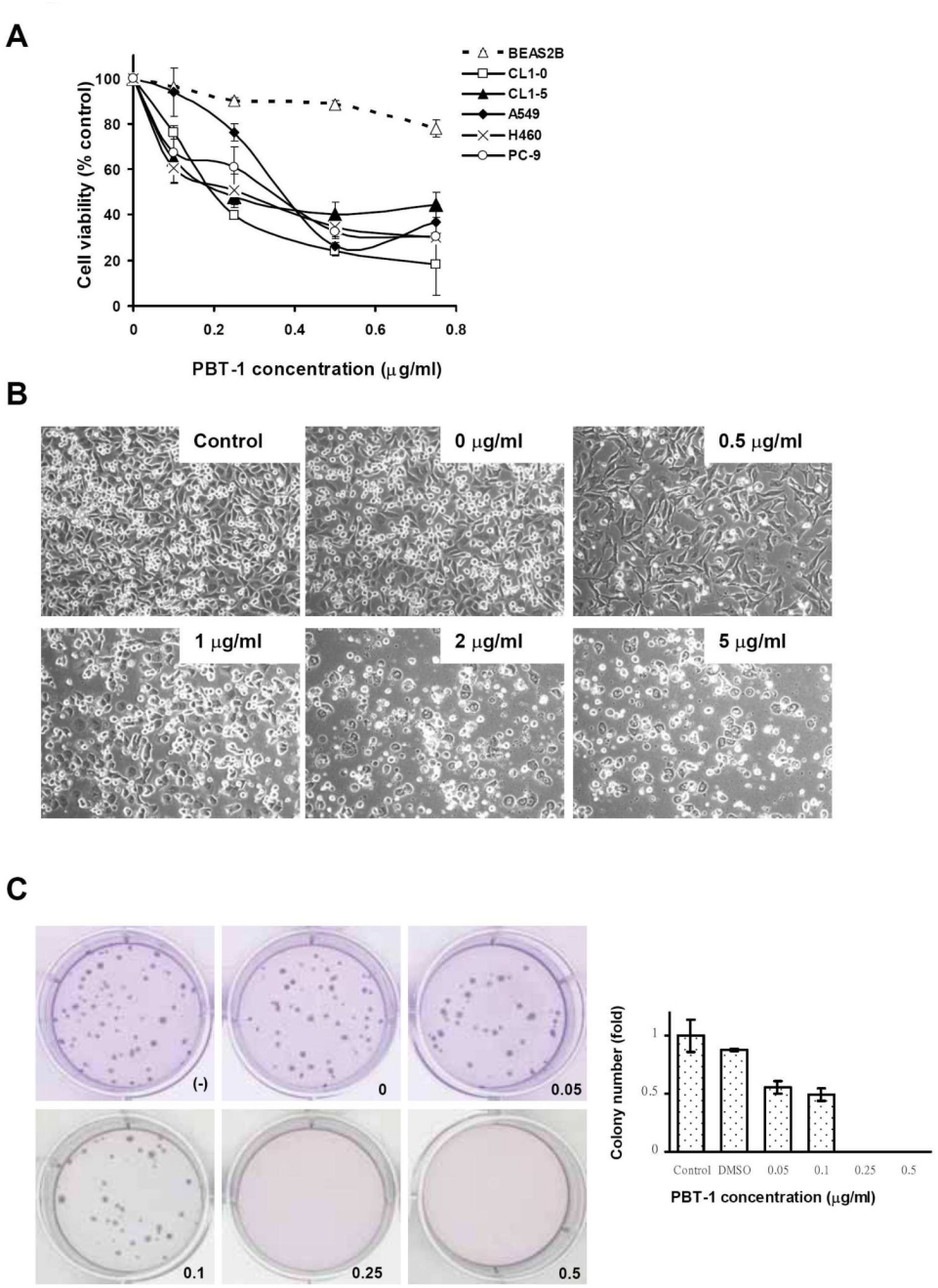

Figure 2. Growth inhibition and loss of clonogenicity in lung cancer cell lines

(A) Various cells were treated with an increasing concentration of PBT-1 of 0, 0.1, 0.25, 0.5, and 0.75 μg/mL for 48 h. The viable cells were detected with an MTS assay. (B) The changes in cell morphology were observed microscopically. The number of viable cells of CL1-5 decreased markedly at a dose of 1 μg/mL of PBT-1. (C) Five hundred cells were plated in soft agar as illustrated with different concentrations of PBT-1 of 0, 0.05, 0.1, 0.25, and 0.5 μg/mL, and then incubated for three weeks. The cells were fixed with 4% paraformaldehyde and stained with 0.01% crystal violet for 16 h. The inhibitory effect of PBT-1 on the colony formation of CL1-0 cells was determined as the percentage of visible colony numbers in the drug-treated groups compared with the untreated control groups. The data are expressed as the mean ± SD.

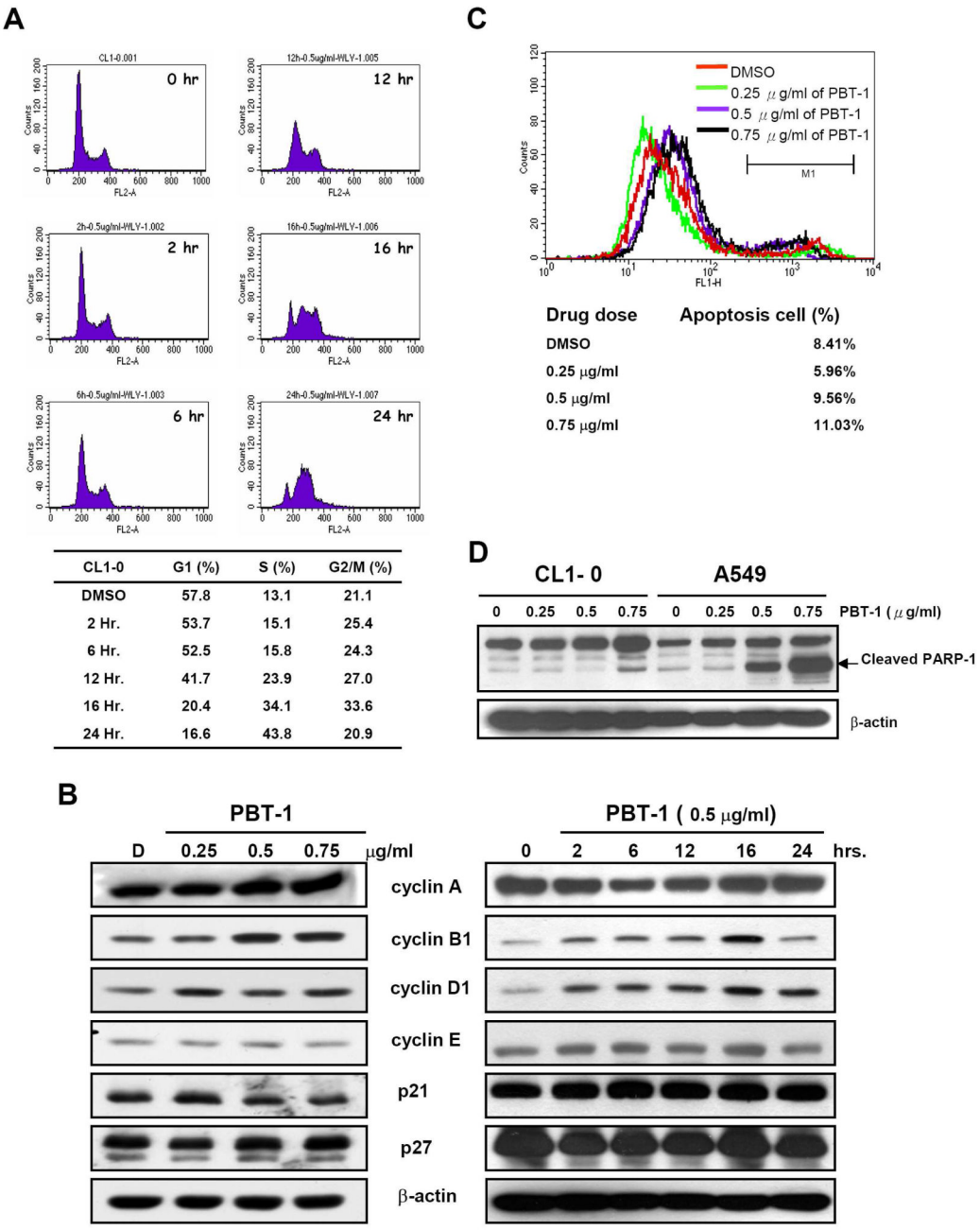

CL1-0	G1 (%)	S (%)	G2/M (%)
DMSO	57.8	13.1	21.1
2 Hr.	53.7	15.1	25.4
6 Hr.	52.5	15.8	24.3
12 Hr.	41.7	23.9	27.0
16 Hr.	20.4	34.1	33.6
24 Hr.	16.6	43.8	20.9

Figure 3. PBT-1 induces cell cycle arrest in G2-M phase and activates apoptotic proteins

(A) CL1-0 cells/dish (2×10^5) were seeded onto each 60 mm dish and incubated for 24 h. Various concentrations of PBT-1 were added to the culture medium and incubated for an additional 2, 6, 12, 16, and 24 h. Cells were then harvested and analyzed by flow cytometry. The cell cycle phase distribution was determined using CellQuest software. (B) CL1-0 cells were treated with increasing concentrations of PBT-1 for 24 h or 0.5 μg/mL for the time indicated. The expression levels of cell cycle regulatory proteins were analyzed by Western blotting. (C) CL1-0 cells were treated with increasing concentrations of PBT-1 for 24 h, stained with Fluor 488 Annexin V and PI, and analyzed by flow cytometry. The percentage of apoptotic

cells is shown in the following table. (D) The expression levels of PARP-1 were analyzed by Western blotting, with actin expression as the internal control.

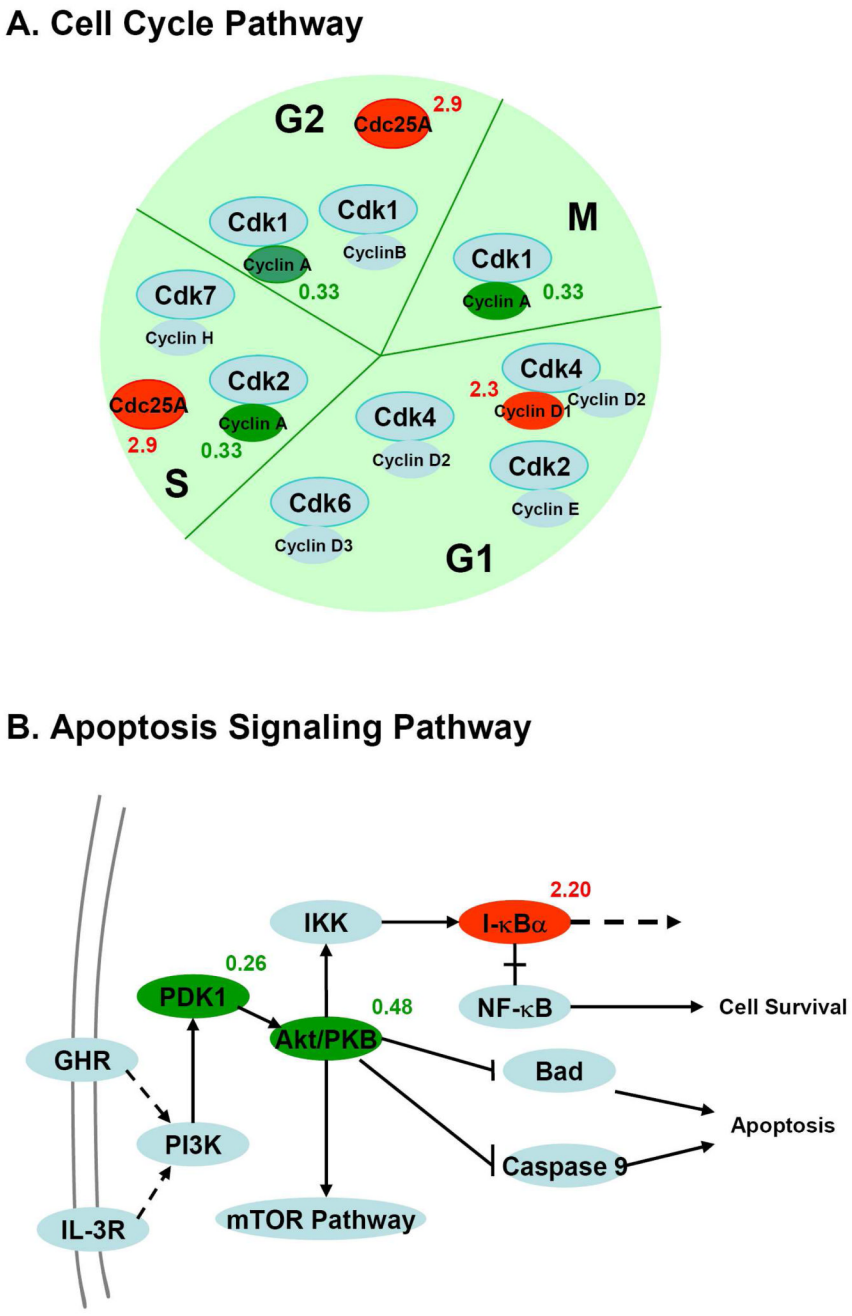

Figure 4.

PBT-1 induced genes in different pathways according to the KEGG and BIOCARTA pathway databases. PBT-1–induced genes are colored red, and the red numbers close to the genes indicate the fold increase. PBT-1–suppressed genes are colored green. (A) Cell cycle pathway. (B) Apoptosis pathway. The hypothetical PBT-1–regulated signaling pathways were modified from the KEGG and BIOCARTA databases.

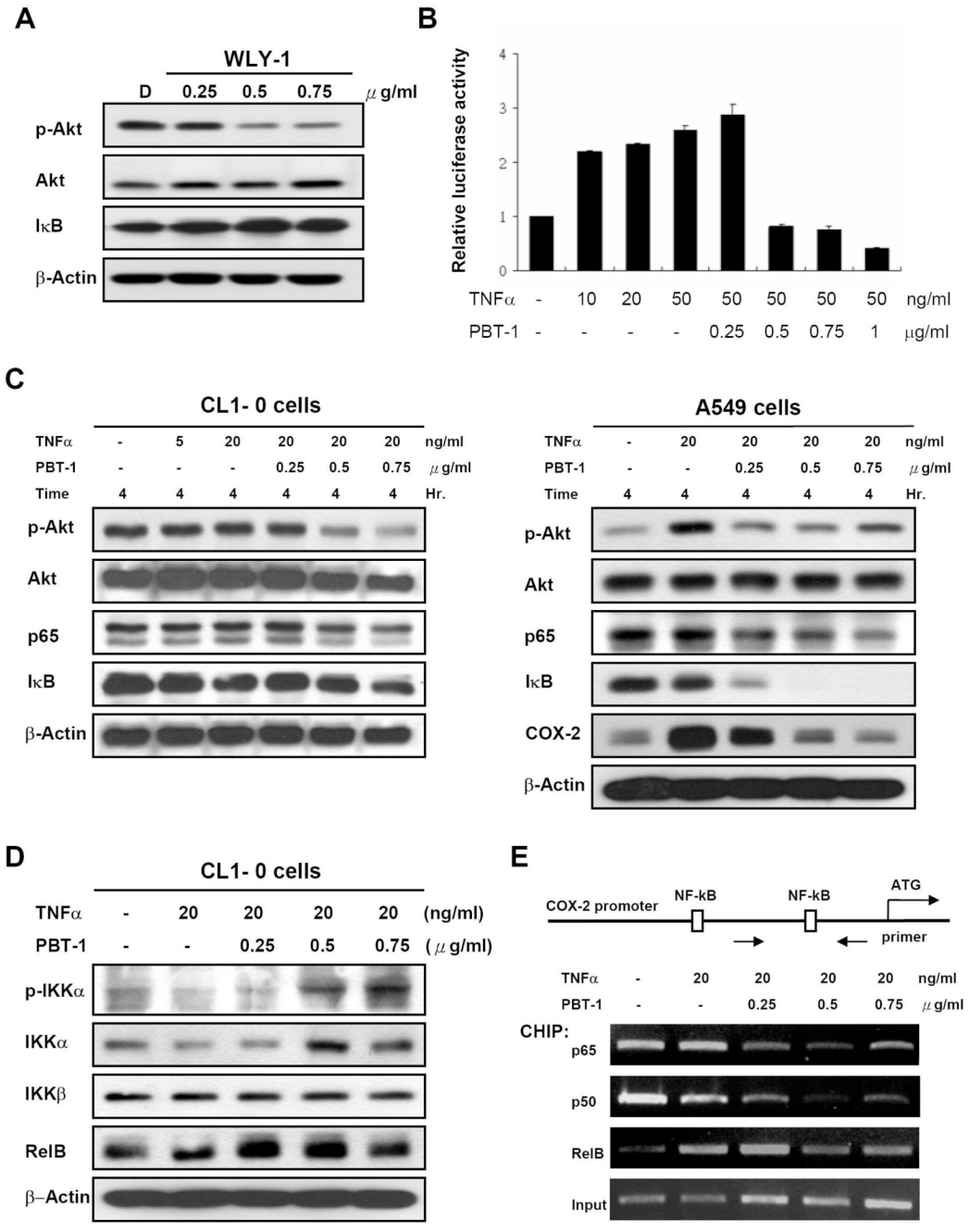

Figure 5. PBT-1 inhibition of the NF-κB signaling pathway correlates with suppression of Akt activity

(A) CL1-0 cells were treated with increasing concentrations of PBT-1 for 24 h. The activity and expression levels of Akt and IκB were analyzed by Western blotting. (B) CL1-0 cells were transiently transfected with pNF-κB-Luc vector and pSV-β-galactosidase vector as the internal control for 20 h. The medium was then changed to serum-free medium without or with increasing concentrations of PBT-1 as indicated for 1 h, and the cells were stimulated with various concentration of TNF-α as indicated for 4 h. The luciferase and β-galactosidase activities were measured using the Luciferase Assay Kit and Galacto-Light Plus™ system. One representative experiment (n=3, independent transfection/treatment) is shown. All data

are presented as mean ± SD. (C, D) CL 1-0 and A549 cells were serum starved overnight, pretreated with various concentrations of PBT-1 as indicated, and then stimulated with TNF-α as indicated for 4 h. The cell extract was probed with specific antibodies as indicated. A representative Western blot is shown. (E) Chromatin immunoprecipitation (ChIP) assays were performed on untreated control A549 cells and on cells treated with PBT-1 and TNF-α as indicated for 4 h. The extracted chromatin was immunoprecipitated with anti-RelA, anti-p50, and anti-RelB antibodies as indicated. The recovered DNA was amplified by PCR using primers covering the region of the *COX2* promoter from nt −359 to +106. Control amplifications were performed on preimmunoprecipitated (“input”) chromatin. A representative ChIP is shown.

Table1

The affected genes related to apoptosis pathway

UniGene	Symbol	Microaray Fold Change Mean ± SD	Molecular function	Real-time PCR Fold Change Mean ± SD	Primers
NM_002730	PRKACA	5.38 ± 2.11	Kinase	1.39 ± 0.31	TCAAACTGATCCAAGTGGGC GCCCTGAGAACAGGACTGAG
NM_003879	CFLAR	3.01 ± 0.68	signal transducer	2.80 ± 0.33	TCAGAATCCTTTCCAGTGGG TCCAGGCTTTCGGTTTCTTT
AL353950	PPP3CA	2.53 ± 0.42	Phosphatase	5.31 ± 0.61	TCCCTCCTTCATAAGATGCG CAATTGATCCCAAGTTGTCG
U72398	BCL2L1	2.70 ± 0.28	Protein binding	1.83 ± 0.17	GGGGTAAACTGGGGTCGCATT ACCTGCGGTTGAAGCGTTC
BC001281	TNFRSF10B	2.53 ± 0.43	Signaling molecular	1.71 ± 0.21	AAGACCCTTGTGCTCGTTGT AGGTGGACACAATCCCTCTG
NM_003954	MAP3K14	2.25	Kinase	2.94 ± 0.61	CCCTTCTCTCACAGCTCCAT ATGGAGGACAAGCAGACTGG
AI078167	NFKBIA	2.23	Protein binding	6.8 ± 0.89	CCATGGTCAGTGCCTTTTCT GTCAAGGAGCTGCAGGAGAT
AF346607	IRAK1	2.1	Kinase	2.23 ± 0.23	GGTGCTTCTCAAAGCCACTC ACACGGACACCTTCAGCTTT
U57843	PIK3CD	2.03	Kinase	1.69 ± 0.25	GGCATCCTGCGTTGTTACTT GACGATAAGGAGTCAGGCC
N32526	AKT3	0.48	Kinase	1.61 ± 0.15	CACTGAAAAGTTGTTGAGGGG AGGTTGGGTTCAGAAGAGGG
AU146532	PDK1	0.26	Kinase	0.56 ± 0.07	GGAGGTCTCAACACGAGGTC GTTCATGTCACGCTGGGTAA